μ^- partial capture rates in ^{16}O

P. Guichon,* B. Bihoreau, M. Giffon,* A. Gonçalves, J. Julien, L. Roussel, and C. Samour
DPh-N/HE, CEN Saclay, BP 2, 91190 Gif-sur-Yvette, France
(Received 12 July 1978)

Using the short pulses of a linac a measurement has been performed of partial μ^--capture rates in ^{16}O leading to the O^- and 1^- bound excited states of ^{16}N. The experimental $O^+ \rightarrow O^-$ transition rate supports the assumption of a large mesonic exchange effect in the time part of the weak axial current.

[NUCLEAR REACTIONS Muon capture $^{16}O(\mu,\nu)^{16}N$. Measured I_γ, Ge(Li) detector. Deduced partial capture rates. Mesonic exchange correction to capture rate calculations.]

I. INTRODUCTION

Interest in muon capture by ^{16}O leading to bound excited states of ^{16}N has existed for a long time.[1-6] Indeed the $0^+ \rightarrow 0^-$ transition is ideally suited to a study of the nuclear weak axial current. The vector part and the spin flip vanish so that the process has a large contribution from the pseudoscalar and timelike parts of the current. Recent microscopic calculations[23,24] show that the time part has a large contribution from the mesonic exchange current while the space part is mainly given by the impulse approximation. Let us emphasize that these calculations rest essentially upon the partially conserved axial current (PCAC) hypothesis, current algebra, and low-energy theorems. So a favorable comparison with experiment is of crucial importance. Because of the large mutual discrepancies among the results of previous muon capture experiments,[7-10] another measurement, made in different conditions, seemed advisable.

Section II gives the principle of the measurement of a muon partial capture rate with the formation of a residual nucleus in an excited state. Section III deals with a short critical discussion of the previous experiments. Section IV describes the experimental setup used at Saclay. Section V presents the data analysis and the results obtained. Section VI contains a tentative theoretical interpretation.

II. PRINCIPLE OF THE MEASUREMENT

The goal of this experiment is to measure the partial capture rates of muons in a K orbit around a ^{16}O target nucleus, that is, the transition rates between the ground state 0^+ of ^{16}O and the bound excited states of ^{16}N (0^-, 120.6 keV) and (1^-, 397.3 keV). The measurement is performed by detecting the two γ rays (120.6 and 276.7 keV) which correspond to the deexcitation of these two states (Fig. 1). Since the branching ratio of the 1^- state is known,[11,12] it is easy to obtain the two partial capture rates $\Lambda_\mu(0^+ \rightarrow 0^-)$ and $\Lambda_\mu(0^+ \rightarrow 1^-)$ from the absolute intensities of the two delayed γ rays. The yield of the prompt $2p \rightarrow 1s$ muonic x-ray (133.5 keV) is used for the absolute normalization.

After the arrival of a muon in the target, the time variation of each nuclear γ ray depends on the lifetime of the muon in K orbit and on the lifetime of the excited state. The 1^- lifetime is very short (42 ± 10 ps), whereas the 0^- state is a metastable one (lifetime 7.58 ± 0.09 μs).[14] Thus the time variation of the 276 keV γ-ray yield depends on the lifetime of the muon in a K orbit around ^{16}O (1.812 ± 0.010 μs),[13] whereas the time variation of the 120 keV γ-ray yield mainly depends on the lifetime of the 0^- state.

The experimental method used to measure such partial capture rates depends on the type of muon beam. In previous experiments[7-9] a quasicontinuous muon beam was used and the γ rays were detected in an observation gate generated each time

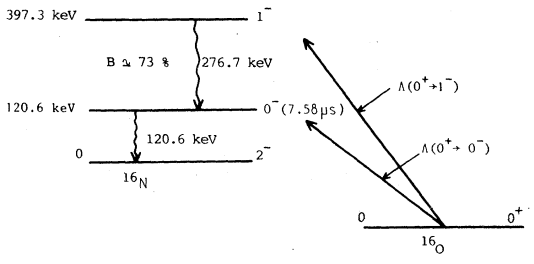

FIG. 1. Partial capture of muons in ^{16}O with the formation of ^{16}N in one of its bound excited states.

a muon was stopped in the target. In this experiment, because of the characteristics of a pulsed linear accelerator, it is possible to produce several muons in a short time interval and to observe the γ rays later in time. Such a method is well adapted to the muon capture in light nuclei, in which the lifetime of a muon is close to 2 μs.

III. PREVIOUS EXPERIMENTS

The partial muon capture rates in ^{16}O have been measured by several groups.[7-10] The various results exhibit large mutual discrepancies, especially for the $0^+ \rightarrow 0^-$ transition (Table I).

The Columbia measurement[7] was performed with a NaI detector. With such a poor resolution detector, the signal-to-noise ratio is low and the γ-line purity may be questionable. The γ rays were detected during a 16 μs gate after the arrival of a single muon in the target.

The Berkeley experiment[8] was also carried out with a NaI detector, but the 276 keV γ ray was detected in correlation with the subsequent 120 keV γ ray in a 34 μs gate. This procedure decreases the background significantly, and at the same time suppresses the contribution of eventual parasite peaks, thus reducing the systematic errors at least for the 276 keV γ ray.

The Louvain experiment[9] was carried out at CERN with a Ge(Li) detector. It was a substantial improvement, but the resolution was still poor compared with the performance of more recent Ge(Li) detectors. Then one cannot rule out a possible contamination of the γ lines by parasite peaks. The γ events were detected in a 6 μs gate opened by each stopped muon.

These three experiments were performed with a quasicontinuous muon beam. As emphasized in Ref. 10, the time gating procedure may induce some ambiguity in the time correlation between a stopped muon and an emitted nuclear γ ray. This ambiguity is suppressed only if the muon beam intensity is very low, as was the case in Ref. 8. Moreover, the very short gate used in Ref. 9 may be questionable for the determination of the 120 keV yield.

In order to avoid the above difficulties, the William and Mary group[10] carried out a measurement with very high resolution detectors without timing requirement. As a consequence the signal-to-noise ratio was poor and there was no information on the time dependence of the γ-ray lines.

The difference between the partial capture rates $\Lambda_\mu(0^+ \rightarrow 0^-)$ and $\Lambda_\mu(0^+ \rightarrow 1^-)$ obtained by these four groups originates from the yields of the observed 120 keV γ ray and of the 276 keV γ ray (Table I). In particular the Louvain group[9] observed a 120 keV yield about 20% lower than the Berkeley[8] and William and Mary groups,[10] while it observed a 276 keV yield about 35% higher than the two other groups.

IV. THE PROCEDURE OF THE PRESENT EXPERIMENT

The problems recalled in Sec. III have led us to perform a measurement under experimental conditions different from the previous ones.[7-10]

A. Muon beam

We have taken advantage of the particular beam structure of the Saclay linac which can deliver short pulses (width $\Delta t = 3.1$ μs) with a repetition rate of 3000 Hz. Under these conditions it is possible to detect the emitted nuclear γ rays during an observation gate $\Delta\theta$ μs which is opened $\Delta\varphi$ μs after the end of the so-called "muon beam pulse" Δt μs (Fig. 5). This method, as in an activation experiment, avoids the regeneration of the μ beam during the measurement. Thereby all ambiguity of time correlation is ruled out. As was already mentioned in Sec. II, this method is well suited to the $1p$-shell nuclei, for which the μ mean life is about 2 μs.

TABLE I. Comparison of the experimental results obtained in the previous measurements.

		Columbia Ref. 7	Berkeley Ref. 8	Louvain CERN Ref. 9	William and Mary Ref. 10
Partial capture rates in s^{-1}	$\Lambda_\mu(0^+ \rightarrow 0^-)$	1100 ± 200	1600 ± 200	850^{+145}_{-60}	1560 ± 180
	$\Lambda_\mu(0^+ \rightarrow 1^-)$	1730 ± 100	1400 ± 200	1850^{+355}_{-170}	1310 ± 110
Yields of the γ rays in 10^{-3} per stopped muon	I(120 keV)	4.16	4.65	3.85	4.46
	I(276 keV)	2.16	1.75	2.31	1.64
	$I(120)/I(276)$	1.92	2.66	1.67	2.73

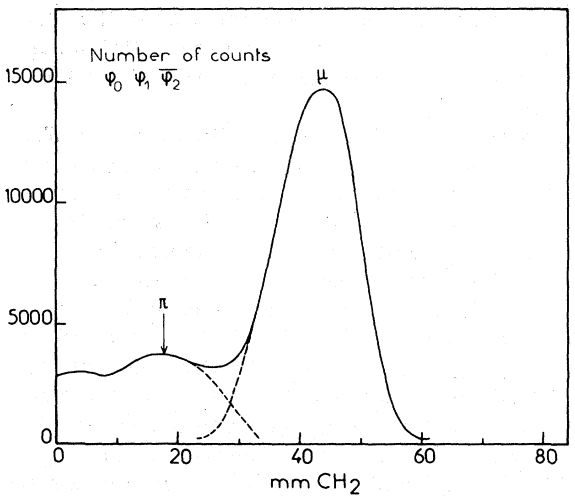

FIG. 2. Differential range curve for the forward muon beam. The FWHM is 1.6 g/cm^2. Ninety percent of the muon beam is stopped in 2 g/cm^2, if the target is centered on the range curve. Pions are stopped in the moderator.

The pion-muon channel PM1 at the Saclay linear accelerator[15] provides 20 MeV backward decay muons or 40 MeV forward decay muons. We have worked with forward muons because they are more intense, while the signal-to-noise ratio remained about the same. The muon incident beam has a 12 cm×7cm (full width at half maximum) [FWHM] section, and the spatial distribution of muons was studied with a ladder scintillation counter. The incident muons were slowed down either in a polyethylene moderator or in a water moderator. Figure 2 shows a typical range curve. Because of the good energy definition of the Saclay muon channel, 90% of the muons can be stopped in a 2 g/cm^2 target, thus reducing the effect of γ absorption. The target thickness was 2 or 3 times lower than that used in Ref. 9. Using the linac conditions, pulse width $\Delta t = 3.1$ μs, repetition rate = 3000 Hz, electron energy = 400 MeV, peak current = 10 mA, it was possible to stop 9000 μ/s in the target. As it can be seen in Fig. 2, the pion contamination is negligible for a 2 g/cm^2 target.

B. Geometry

The target consisted of distilled water enclosed in a disc container made of plexiglass, having a diameter of 20 cm and a thickness of 2 cm. The frontal windows of this container had a thickness of 0.3 mm. The angle between the incident muon beam axis and the cylinder axis was ~20° (Fig. 3).

The γ-ray detector was a coaxial Ge(Li) detector of 80 cm^3 (manufactured by Quartz-et-Silice) with a resolution (FWHM) of 1 keV at 120 keV. Its efficiency has been studied with various standard sources (for instance ^{152}Eu and monazite sample) with the method described in Ref. 16. The relative efficiency versus energy was known with a precision of 1% in the region of interest. It has been checked with muonic x-ray spectra from water, magnesium, and iron samples. Our results are in agreement with those of Ref. 17–19. Some additional checks have been made with two other detectors, the first one was a 100 cm^3 coaxial Ge(Li) detector (manufactured by Quartz-et-Silice), the second one was a 1.5 cm^3 hyperpure Ge detector (manufactured by ORTEC).

Figure 3 shows the apparatus setup. The detector was shielded with a lead collimator. The geometry is of crucial importance in such an experiment and we made a careful study of its influence by changing the positions of the collimator, moderator, target, and detector. The geometry drawn in Fig. 3 gave the best signal-to-noise ratio. The latter depends very critically on the position of the detector. This one must be set very close to the target, but it must see neither the moderator nor the pion-muon channel output. The angle between the target and the Ge(Li) front plane was ~40°.

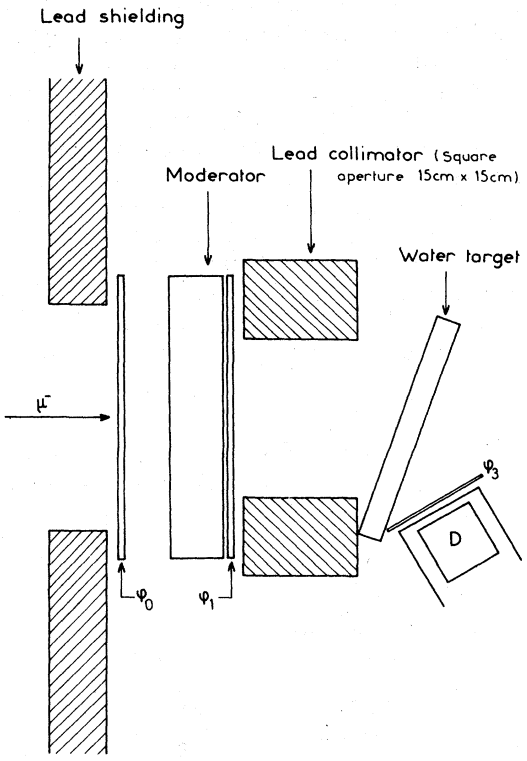

FIG. 3. Experimental setup.

The muon beam was controlled by three plastic scintillators ϕ_0, ϕ_1, and ϕ_2. The dimensions of ϕ_0 and ϕ_1 were 20 cm×20 cm×3 mm, and those of ϕ_2 were 25 cm×25 cm×4 mm. An incident charged particle (muon or contamination electron) was defined by the coincidence ϕ_0, ϕ_1, a stopped muon was defined by the coincidence-anticoincidence ϕ_0, ϕ_1, $\overline{\phi}_2$, the ϕ_2 scintillator (not represented in Fig. 3) is placed just after the target. This last counter has been removed during the runs. Another scintillator ϕ_3 (10 cm×10 cm×2 mm) in front of the Ge(Li) detector D is used to distinguish between the charged and neutral particles emitted by the target and detected by the Ge(Li).

C. Data recording

The time distributions of the incident charged particles, stopped muons, charged particles in the Ge(Li), and neutral particles in the Ge(Li) were defined by the delay times of $\phi_0\phi_1$, $\phi_0\phi_1\overline{\phi}_2$, $\phi_3 D$, and $\overline{\phi}_3 D$ signals with respect to a triggering signal S during a 40 μs gate G (Fig. 5). The signal S was given by the linac logic system before the beginning of each electron beam pulse. The $\phi_0\phi_1$ and $\phi_0\phi_1\overline{\phi}_2$ time distributions were quite similar and only the first one was recorded during the runs. We have also verified that the time distribution of the muonic x rays detected in the Ge(Li) was the same. In Fig. 4 we show the distribution for $\phi_0\phi_1$ from which we define the so-called gate Δt (Fig. 5). This distribution has been used to compute with precision the timing correction to the 120 and 276 keV γ-ray yields.

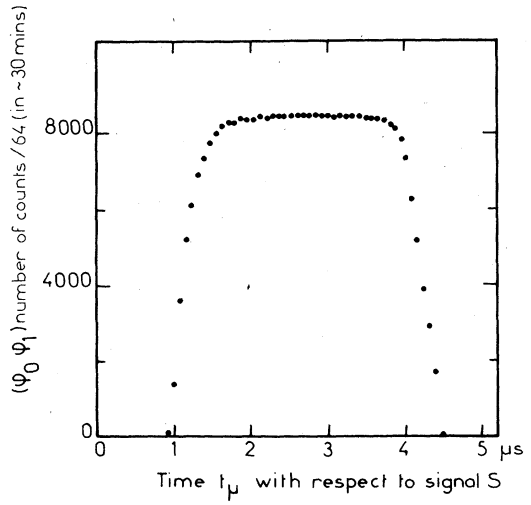

FIG. 4. Time distribution of incident charged particles. The time distributions of stopped muons and 133 keV x rays are quite similar.

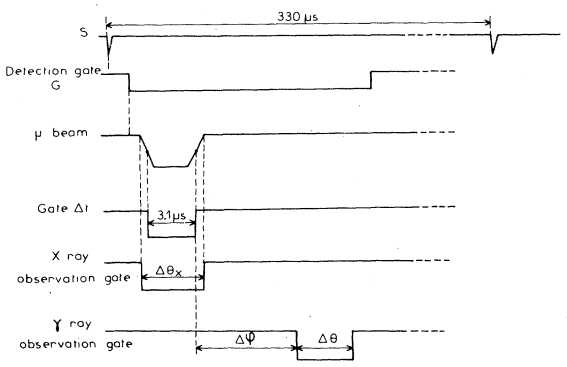

FIG. 5. Timing diagram explaining our experimental method. From the muon distribution of Fig. 4 we define arbitrarily a so-called "muon gate" Δt taken from the FWHM of this distribution. The time intervals $\Delta\varphi$ and $\Delta\theta$ are defined with respect to this gate Δt. Muonic x rays and nuclear γ rays are detected in the gate G = 40 μs. Muonic x rays are emitted during the gate $\Delta\theta_X$ corresponding to the total muon distribution. During the analysis of the data we choose an observation gate $\Delta\theta$ for the nuclear γ rays such that the signal-to-noise ratio is the best possible.

All the data were recorded with a PDP 15/30 computer via a CAMAC system. The pulse height of the Ge(Li) detector signal was analyzed with a Tennelec TC-203 BLR amplifier and a Schlumberger JCAN-21 C amplitude converter. For the muon capture experiment we have taken 0.3 keV/channel. The timing of the Ge(Li) was given by an ORTEC-454 amplifier and an ORTEC-473A discriminator. The time resolution (FWHM) of the Ge(Li) with respect to ϕ_3 was 6 ns for a particular choice of ORTEC-454 amplifier time constants. The time delays between the occurrence of signal S and the signals $\phi_3 D$, $\overline{\phi}_3 D$, $\phi_0\phi_1$, and $\phi_0\phi_1\overline{\phi}_2$ were analyzed in 32 000 channel 1000 MHz digitrons (manufactured by L.E.T.I. at CEN Grenoble) whose channel width was 2 ns (with a precision of 2×10^{-5}). To maintain the Ge(Li) resolution and avoid electronic and computer dead-time effects we have limited the linac electron peak current to 10 mA so that the Ge(Li) counting rate was 0.15 per linac pulse.

V. DATA ANALYSIS AND DISCUSSION

A. The nuclear γ-ray events

Since each γ-ray event $\overline{\phi}_3 D$ is characterized by its pulse height (energy) and its detection time, it was possible to choose the observation gate $\Delta\theta$ (Fig. 5) corresponding to the best signal-to-noise ratio during the analysis of the data. The maximum ratio was obtained under the following con-

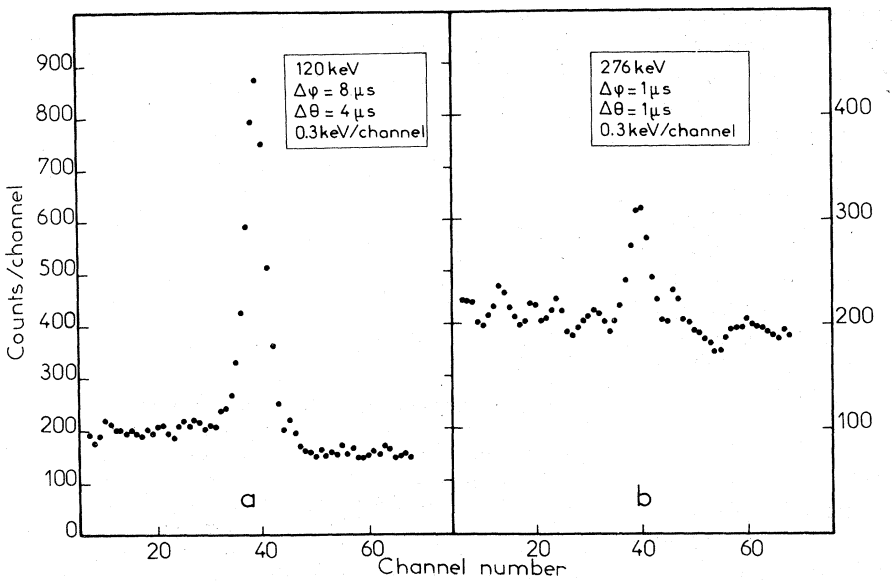

FIG. 6. Spectra obtained for the 120 keV (part a) and the 276 keV (part b) for the particular observation gates $\Delta\theta$ which gives the maximum signal-to-noise ratios. They are $\Delta\varphi = 8\ \mu$s, $\Delta\theta = 4\ \mu$s for the 120 keV and $\Delta\varphi = 1\ \mu$s, $\Delta\theta = 1\ \mu$s for the 276 keV.

ditions: $\Delta\varphi = 8\ \mu$s, $\Delta\theta = 4\ \mu$s for the 120 keV γ ray and $\Delta\varphi = 1\ \mu$s, $\Delta\theta = 1\ \mu$s for the 276 keV γ ray. Figure 6 shows the corresponding spectra. Figure 6(a) illustrates the γ ray from the decay of the 0^- isomeric state at 120 keV in ^{16}N (Fig. 1). Because of the mean life of this state, it is a particularly favorable case. Indeed the signal-to-noise ratio is excellent for an observation gate $\Delta\theta$ placed far away from the Δt pulse. Figure 6(b) shows the $1^- \rightarrow 0^-$ γ transition. The mean life of the 396 keV 1^- state is very short, and the 276 keV γ line has an apparent mean life equal to that of a K-orbit muon and the gate $\Delta\theta$ must be chosen closer to gate Δt. For these two γ rays the resolution (FWHM) for all the data is 1.2 keV. During the experiment we observed a slight and slow variation of the gain and threshold of the GeLi pulse height spectrum, due to a temperature instability. Indeed the resolution of the whole data without any correction was 1.5 keV. To counteract this effect the data were divided into partial runs, each of them corresponding to a 30 min recording. A shifting routine[20] was designed which calculated the centroids of two reference γ rays (the 133 keV muonic x ray and the 511 keV e^+-annihilation γ line) and placed them in the same channels.

Let us note that the 276 keV γ ray cannot be broadened by Doppler effect, where the mean life of the 1^- state is sufficiently long (~40 ps) with respect to the slowing down time of the recoil nucleus (~1 ps). As shown in Fig. 7 we have verified that the time variation of the two γ intensities follows their appropriate mean life. Moreover,

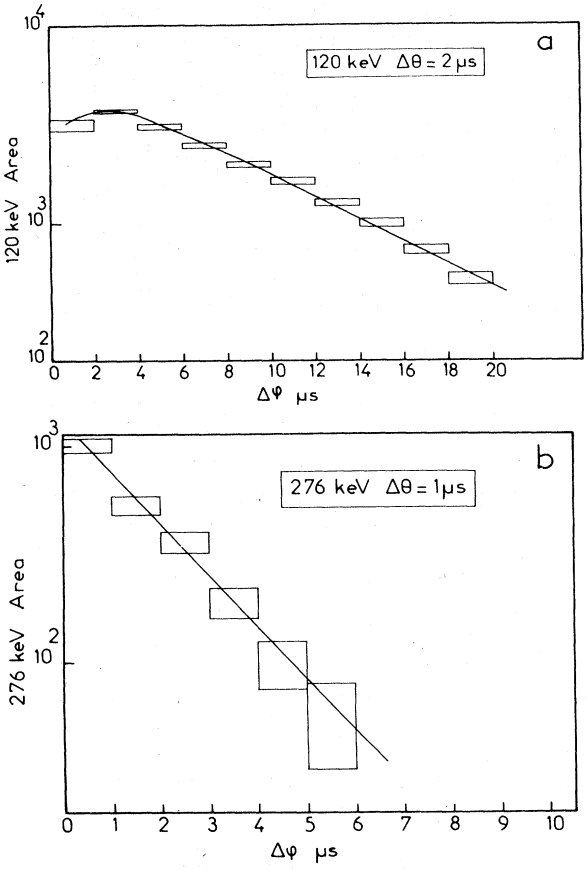

FIG. 7. Time dependence of the 120 keV (part a) and 276 keV (part b) γ-ray lines. The binning width was, respectively, 2 and 1 μs. The solid curves show the expected time dependences.

the time variation of the muon decay electrons detected by $\phi_0\phi_1$ and $\phi_3 D$ just after the muon pulse is compatible with the mean life of muons in a K orbit around ^{16}O.

B. Background

The smooth background in the γ spectra has two major sources. The first one is due to the bremsstrahlung of the muon decay electrons induced in the target and in the various materials surrounding the detector. The second one is due to the Compton contribution of higher energy γ rays induced by reactions (n,γ) or $(n,n'\gamma)$ in the surrounding materials. These neutrons have several origins. They can arise from the copper conversion target in which the linac electron beam produces the pion beam. They are also produced by the pions in the last bending magnet of the channel, by the muons in the collimator and in the target, and by the bremsstrahlung in the surrounding materials. The importance of the neutron background was put in evidence in another experiment of partial muon capture in a ^{10}B target. Indeed we have observed the well-known 480 keV γ ray due to the reaction $^{10}\mathrm{B}(n,\alpha)$, for which the cross section is very high for low-energy neutrons. A complete discussion will be given in another paper.[21]

In the time variation of the γ background near the 120 keV γ ray and near the 276 keV γ ray for the water target, we observed a mixing of several mean lives. However, with the small number of points and the statistics we have, it is impossible to separate them clearly. Some parasite peaks which appear in the γ-energy spectra are probably induced by the background neutrons. They also appeared with a graphite target. In particular we observed two peaks on each side of the 276 keV γ ray at 274 and 278 keV, which have not been identified. We also note the presence of the 122 and 136 keV lines induced by the reaction $^{56}\mathrm{Fe}(n,\gamma)$.

It is clear that such an experiment must be performed with a high resolution detector and that the background must be carefully studied with a different target element, because the time dependence of one γ-ray line is not a sufficient test to affirm that there is no contamination. Let us emphasize that if we had taken an energy interval of 4 or 5 keV as in Ref. 9 to evaluate the 276 keV area, the result would have been changed by 25%.

C. Role of the (n,p) secondary process

Another confusion, already noted in Ref. 7, may arise from possible (n,p) reactions induced in the target itself by sufficiently energetic neutrons produced by muon capture in ^{16}O. Nevertheless most of these neutrons have a low energy[22] and the threshold of the reaction $^{16}\mathrm{O}(n,p)^{16}\mathrm{N}$ is high ($Q=-9.6$ MeV).[14] In any case this secondary effect should depend quadratically on the target thickness. Comparison of 120 keV intensities obtained with two target thicknesses (1 g/cm^2 and 2 g/cm^2) did not show any difference, in agreement with the conclusion of Ref. 7.

D. Evaluation of the capture rates

The capture rates $\Lambda_\mu(0^+ \to 0^-)$ and $\Lambda_\mu(0^+ \to 1^-)$ are evaluated from the yield of the 120 and 276 keV γ rays obtained, respectively, for the following time conditions: $\Delta\varphi = 4\ \mu$s, $\Delta\theta = 14\ \mu$s for the 120 keV and $\Delta\varphi = 0$, $\Delta\theta = 6\ \mu$s for the 276 keV. The corresponding spectra are given in Fig. 8. We have checked that the final results are independent of the timing conditions we have chosen.

The absolute normalization is determined from the total $K(np \to 1s)$ (that is, the so-called Lyman series) yield. Then it does not necessitate the knowledge of the total number of muons which stopped in the target. This assumes that each stopped muon gives one K muonic x ray. This normalization method is well suited to our case because the γ-ray lines and the muonic x rays have about the same energy. The relative intensity of the $2p \to 1s$ transition is evaluated from the Lyman series, and then provides a secondary yield standard for the γ-ray data. Figure 9 shows the x-ray spectra and Table II gives the relative intensities of the K x rays in ^{16}O. The results are in good agreement with those of Ref. 19.

During the gate $\Delta\theta_X$ when the x rays were observed (Fig. 5) the counting rate was higher than during any delayed gate $\Delta\theta$. It was therefore necessary to verify with a pulse generator that the deadtime of the logic system did not depend on the position of the observation gate.

We made a correction for the self absorption of x rays and γ rays in the target and in the scintillator ϕ_3, taking into account the spatial distribution of the stopped muons. This correction has been checked with radioactive sources set behind an equivalent water screen, and further confirmation was obtained from the comparison of ^{16}O muonic x-ray yields in a 2 g/cm^2 water target and in a 1 g/cm^2 target.

Finally we must make a timing correction for the 120 and 276 keV γ rays. For this we use the time distribution of the stopped muons shown in Fig. 4. Indeed because the nuclear γ rays are observed in a finite delayed interval of time, a correction must be made for those events which are not observed.

The two partial capture rates $\Lambda_\mu(0^+ \to 0^-)$ and

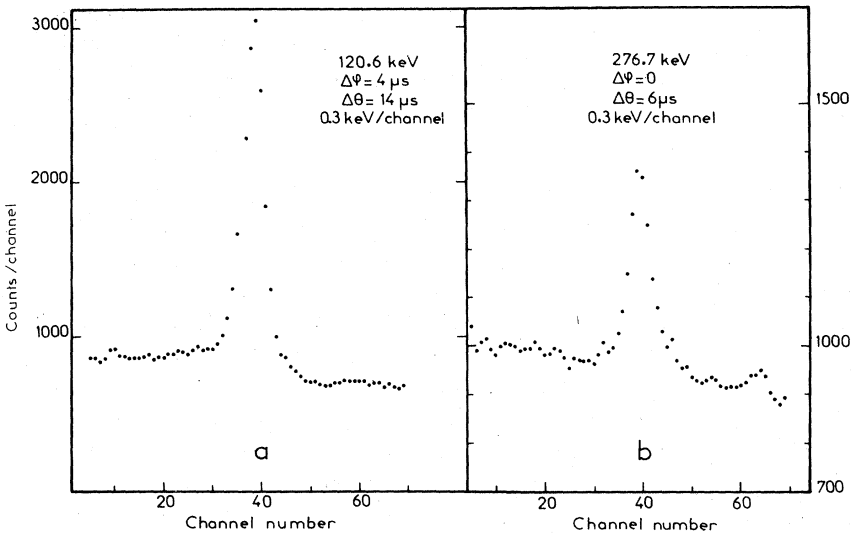

FIG. 8. ^{16}O γ data from which the peak areas were calculated and the partial rates estimated. The timing conditions are $\Delta\varphi = 4$ μs, $\Delta\theta = 14$ μs for the 120 keV γ ray and $\Delta\varphi = 0$, $\Delta\theta = 6$ μs for the 276 keV γ ray. So for this latter γ ray the observation gate begins before the end of the real muon distribution.

TABLE II. Energies and relative intensities of the muonic x ray Lyman series for ^{16}O. Intensity ratios multiplied by 10^3 are given. The errors shown include all errors (statistics, efficiency and transmission).

x ray	Energy keV	Relative intensity	
$K\alpha$	133.5	$K\alpha/K\alpha = 1000$	$\lambda_{133} \equiv K\alpha/\text{total} = 573(\pm 0.4\,\%)$
$K\beta$	158.4	$K\beta/K\alpha = 312(\pm 1.4\,\%)$	
$K\gamma$	167.1	$K\gamma/K\alpha = 261(\pm 1.4\,\%)$	
$K\delta$	171.1	$K\delta/K\alpha = 128(\pm 1.6\,\%)$	
$K\epsilon$	173.3	$K\epsilon/K\alpha = 44(\pm 4.5\,\%)$	

TABLE III. Values and errors of the different quantities entering in the calculation of the intensities I_{120} and I_{276}.

	I_{120}	I_{120}/I_{276}
Area [a]	$A_{120} = 12\,061(\pm 1.15\,\%)$	$A_{120} = 12\,061(\pm 1.15\,\%)$
	$A_{133} = 2\,745 \times 10^3(\pm 0.1\%)$	$A_{276} = 2\,244(\pm 4.8\,\%)$
	$\frac{A_{120}}{A_{133}} = 4.39 \times 10^{-3}(\pm 1.15\,\%)$	$\frac{A_{120}}{A_{276}} = 5.37(\pm 5\,\%)$
Efficiency	$\frac{\epsilon_{133}}{\epsilon_{120}} = 0.925(\pm 1.4\,\%)$	$\frac{\epsilon_{276}}{\epsilon_{120}} = 0.525(\pm 1.4\,\%)$
Transmission	$\frac{t_{133}}{t_{120}} = 1.008(\pm 0.4\,\%)$	$\frac{t_{276}}{t_{120}} = 1.074(\pm 4\,\%)$
Timing [a]	$\frac{\theta_{133}}{\theta_{120}} = 1.921(\pm 0.5\,\%)$	$\frac{\theta_{276}}{\theta_{120}} = 0.886(\pm 0.5\,\%)$
Normalization	$\lambda_{133} = 0.573(\pm 0.4\,\%)$	
Total	$I_{120} = (4.51 \pm 0.09) \times 10^{-3}$	$\frac{I_{120}}{I_{276}} = 2.68 \pm 0.18$

[a] With $\Delta\varphi = 4$ μs, $\Delta\theta = 14$ μs for 120 keV γ ray, and with $\Delta\varphi = 0$, $\Delta\theta = 6$ μs for 276 keV γ ray.

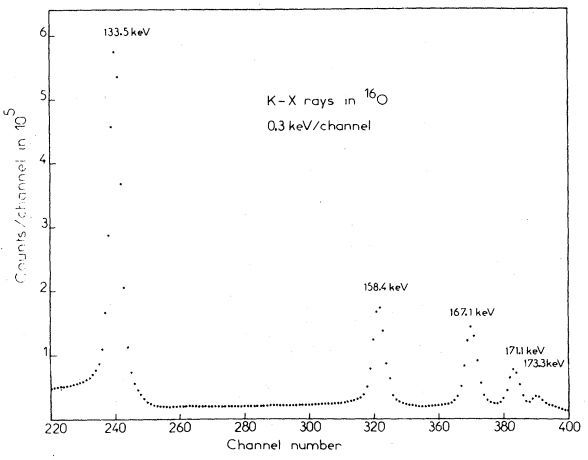

FIG. 9. Muonic x-ray spectra for ^{16}O target.

$\Lambda_\mu(0^+ \to 1^-)$ are related to the 120 and 276 keV γ-ray areas by the following relations:

$$A_{120} = \phi_\mu \epsilon_{120} \Omega t_{120} \theta_{120} \frac{\Lambda_\mu(0^+ \to 0^-) + B\Lambda_\mu(0^+ \to 1^-)}{\Lambda_{\mu\,\text{total}}} ,$$

$$A_{276} = \phi_\mu \epsilon_{276} \Omega t_{276} \theta_{276} \frac{B\Lambda_\mu(0^+ \to 1^-)}{\Lambda_{\mu\,\text{total}}} ,$$

where ϕ_μ is the total number of stopped muons, ϵ is the Ge-Li efficiency, Ω is the solid angle, t is the transmission factor, and θ is the timing correction. $\Lambda_{\mu\,\text{total}}$ is the muon disappearance rate $\Lambda_{\mu\,\text{total}} = (5.519 \pm 0.030) \times 10^5\ \text{s}^{-1}$.[13]

ϕ_μ is obtained from the $2p \to 1s$ muonic x-ray area

$$A_{133} = \phi_\mu \epsilon_{133} \Omega t_{133} \theta_{133} \lambda_{133} ,$$

where $\theta_{133} = 1$, the x rays are observed in the gate $\Delta\theta_X$ (Fig. 5). λ_{133} is the relative intensity of the $2p \to 1s$ transition in the total Lyman series (Table III).

Then we have

$$\frac{A_{120}}{A_{133}} = \frac{\epsilon_{120}}{\epsilon_{133}} \frac{t_{120}}{t_{133}} \frac{\theta_{120}}{\theta_{133}} \frac{1}{\lambda_{133}} \frac{\Lambda_\mu(0^+ \to 0^-) + B\Lambda_\mu(0^+ \to 1^-)}{\Lambda_{\mu\,\text{total}}} ,$$

$$\frac{A_{120}}{A_{276}} = \frac{\epsilon_{120}}{\epsilon_{276}} \frac{t_{120}}{t_{276}} \frac{\theta_{120}}{\theta_{276}} \frac{\Lambda_\mu(0^+ \to 0^-) + B\Lambda_\mu(0^+ \to 1^-)}{B\Lambda_\mu(0^+ \to 1^-)} .$$

We introduce the intensities I_{120} and I_{276}, that is, the number of 120 keV γ rays and of 276 keV γ rays per stopped muons:

$$I_{120} = \frac{A_{120}}{A_{133}} \frac{\epsilon_{133}}{\epsilon_{120}} \frac{t_{133}}{t_{120}} \frac{\theta_{133}}{\theta_{120}} \lambda_{133} ,$$

$$\frac{I_{120}}{I_{276}} = \frac{A_{120}}{A_{276}} \frac{\epsilon_{276}}{\epsilon_{120}} \frac{t_{276}}{t_{120}} \frac{\theta_{276}}{\theta_{120}} .$$

TABLE IV. Saclay partial capture rates.

Transition	Branching ratio B	Capture rate in s^{-1}
$0^+ \to 0^-$		1560 ± 108
$0^+ \to 1^-$	0.69 ± 0.05 [a]	1345 ± 135
	0.734 ± 0.016 [b]	1265 ± 92

[a] Value given in Ref. 11 and taken in Refs. 7–10.
[b] Value given in Ref. 12.

Since only the ratios of efficiency, transmission, and timing of the γ rays occur in the calculation, the errors are minimized. Table III gives the various parameters and their errors.

Finally we have

$$\Lambda_\mu(0^+ \to 0^-) = \Lambda_{\text{total}}(I_{120} - I_{276}) = \Lambda_{\text{total}} I_{120} \left(1 - \frac{I_{276}}{I_{120}}\right) ,$$

$$\Lambda_\mu(0^+ \to 1^-) = \Lambda_{\text{total}} \frac{I_{276}}{B} = \Lambda_{\text{total}} \frac{I_{120}}{B} \frac{I_{276}}{I_{120}} .$$

Two values of the 1^- state branching ratio B were used,[11,12] to calculate the partial capture rates which are given in Table IV. Our results are in agreement with the Berkeley[8] and the William and Mary[10] results.

VI. TENTATIVE INTERPRETATION

The interpretation of the muon capture rate encounters two problems. The first one is the approximate character of the nuclear state description provided by the truncated shell model. One can get rid of this problem if the inverse process (β^- decay) is available.[25] Indeed the shortcomings of the nuclear model should cancel to a large extent when one takes the ratio of the theoretical muon capture and β-decay rates. Unfortunately the trick works only for the $0^+ \to 0^-$ transition, while for the $0^+ \to 1^-$ transition we must be content with phenomenological wave functions[26] which have been fitted to reproduce energy and electromagnetic transition rate of the isobaric analog state.

The second problem is the questionable validity of the so-called impulse approximation (IA). An extremely confusing way to phrase the problem is that a nucleon inside the nuclear medium has not the weak coupling constants of a free nucleon. It is not our purpose to discuss the renormalization effect, and we refer the reader to specialized papers.[27,28] However, we must recall some basic facts that are necessary for an understanding of the interpretation of our experiment.

Generally speaking any renormalization arises

from some truncation of the model space one uses to compute matrix elements. In the IA the model space is spanned by the A nucleons (A is the nucleus mass number) without any reference to the possible "nucleons + mesons" virtual states. The use of wave functions constructed from some phenomenological potential together with the use of the free nucleon coupling constants takes only partial account of this shortcoming. There are situations where this treatment is to some extent correct. In the long wavelength limit (this involves 20 or 30% error in μ capture) the Siegert theorem ensures that virtual meson states do not contribute to the electric multipoles of the weak vector current. Thus the vector part of the $0^+ \to 1^-$ transition can be evaluated in the IA without a large error. A similar statement does not hold for the weak axial current and corrections to the IA are necessary. We do not go into details because the description of mesonic exchange corrections to the axial current can be found elsewhere.[23,29,30] Of course the meson exchange corrections involve at least the coordinates of two nucleons. Thus the introduction of renormalized coupling constants[31] implies averaging over the coordinates of all the nucleons but one. Because the result depends on the particular transition studied, the procedure is of little use.[32] It is perfectly equivalent to compute directly the matrix elements of the two (or many) body operators corresponding to the mesonic corrections and to add them to the IA matrix elements. It is this last method we have used in Refs. 23, 24 and, as it should be clear, the weak coupling constants in the IA part must be the free ones.[34]

The mesonic exchange effect has been evaluated in the one-pion exchange (OPE) approximation and the Adler-Dothan result[35] has been used for the weak axial pion production amplitude. Thus our correction to the IA is founded on the current algebra and PCAC hypothesis together with low energy techniques. All matrix elements have been evaluated in the Tamm-Dancoff particle-hole approximation (TDA), with a hole in the $1p$ shell and a particle in the $2s$-$1d$ shell around a closed core of ^{16}O. It turns out that the spacelike part of the axial current is negligibly affected by exchange currents.[23] Another calculation,[33] including pion rescattering effect, agrees with this result. For this reason and because some doubts have been cast on the OPE approximation for the space part of the axial current[36] we prefer to neglect it completely in our analysis.

Thus the $0^+ \to 1^-$ transition, independent of the timelike part of the axial current, should be described by the IA with the wave functions of Ref. 26 and with the canonical values of the weak cou-

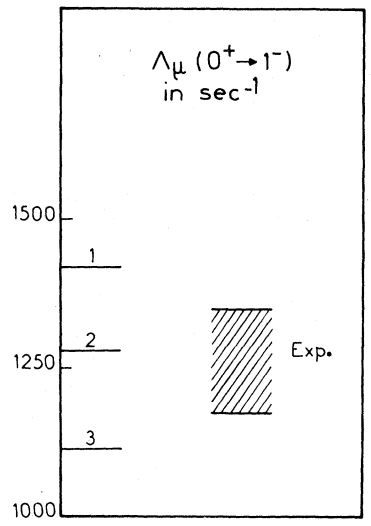

FIG. 10. The experimental value of $\Lambda_\mu(0^+ \to 1^-)$ is compared with the analysis of Donnelly and Walecka based on electron scattering. Results 1 and 2 are obtained, respectively, in the TDA and random-phase approximation (RPA) with harmonic oscillator wave functions. Result 3 is obtained in the TDA with Wood-Saxon wave functions.

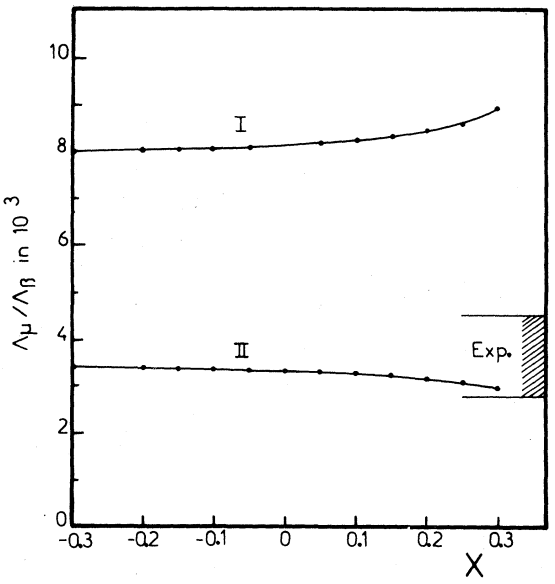

FIG. 11. Variation of the ratio $\Lambda_\mu(0^+ \to 0^-)/\Lambda_\beta(0^- \to 0^+)$ as a function of the mixing coefficient X for the $(1p_{3/2}^{-1}, 1d_{3/2})$ component. The curve I corresponds to the impulse approximation, the curve II includes the mesonic exchange correction. The experimental ratio (exp) was evaluated from the present muon-capture experiment $\Lambda_\mu(0^+ \to 0^-) = 1560 \pm 108$ s^{-1} and from the Louvain β-decay experiment (Ref. 38) $\Lambda_\beta(0^- \to 0^+) = 0.43 \pm 0.10$ s^{-1}.

pling constants.[34] There is agreement between theory and experiment (Fig. 10). This gives qualitative support to the fact that the space part of the axial current is little affected by exchange currents. No more information can be obtained from this transition for the moment.

The $0^+ \to 0^-$ transition has a large contribution from the timelike part of the axial current and, as shown in Refs. 23 and 24, this part is strongly affected by OPE correction. The matrix element is changed from its IA value by a factor ~1.5. An important point is that this factor practically does not depend on the nuclear model. An estimation made in the Fermi gas model[37] gives about the same value. As a consequence the nuclear model uncertainties are of importance only for the IA part. In order to minimize these uncertainties we have computed the ratio of muon capture rate $\Lambda_\mu(0^+ \to 0^-)$ to beta decay rate $\Lambda_\beta(0^- \to 0^+)$. Ratio I is evaluated in the IA. Ratio II is evaluated with a OPE correction to the timelike part of the axial current for both muon capture and β decay. (Again we neglect corrections to the space part.) There are only two possible configurations for the 0^- state ($1p_{1/2}^{-1}2s_{1/2}$ and $1p_{3/2}^{-1}1d_{3/2}$). In Fig. 11 are plotted ratios I and II versus the mixing parameter X together with the experimental ratio. The latter was computed from our $\Lambda_\mu(0^+ \to 0^-)$ experimental value and the $\Lambda_\beta(0^- \to 0^+)$ experimental value of Ref. 38.

Ratios I and II are quite independent of the mixing parameter X, though we have extended its variation up to unrealistic values. The agreement between the experimental ratio and ratio II is quite good.

Of course care must be taken before concluding in favor of this interpretation. First of all, $\Lambda_\beta(0^- \to 0^+)$ should be measured with a greater accuracy, because it is the main source of uncertainty in Fig. 11. Furthermore one should verify that, by extending the nuclear model to configurations of higher energy, the result is not changed. More-

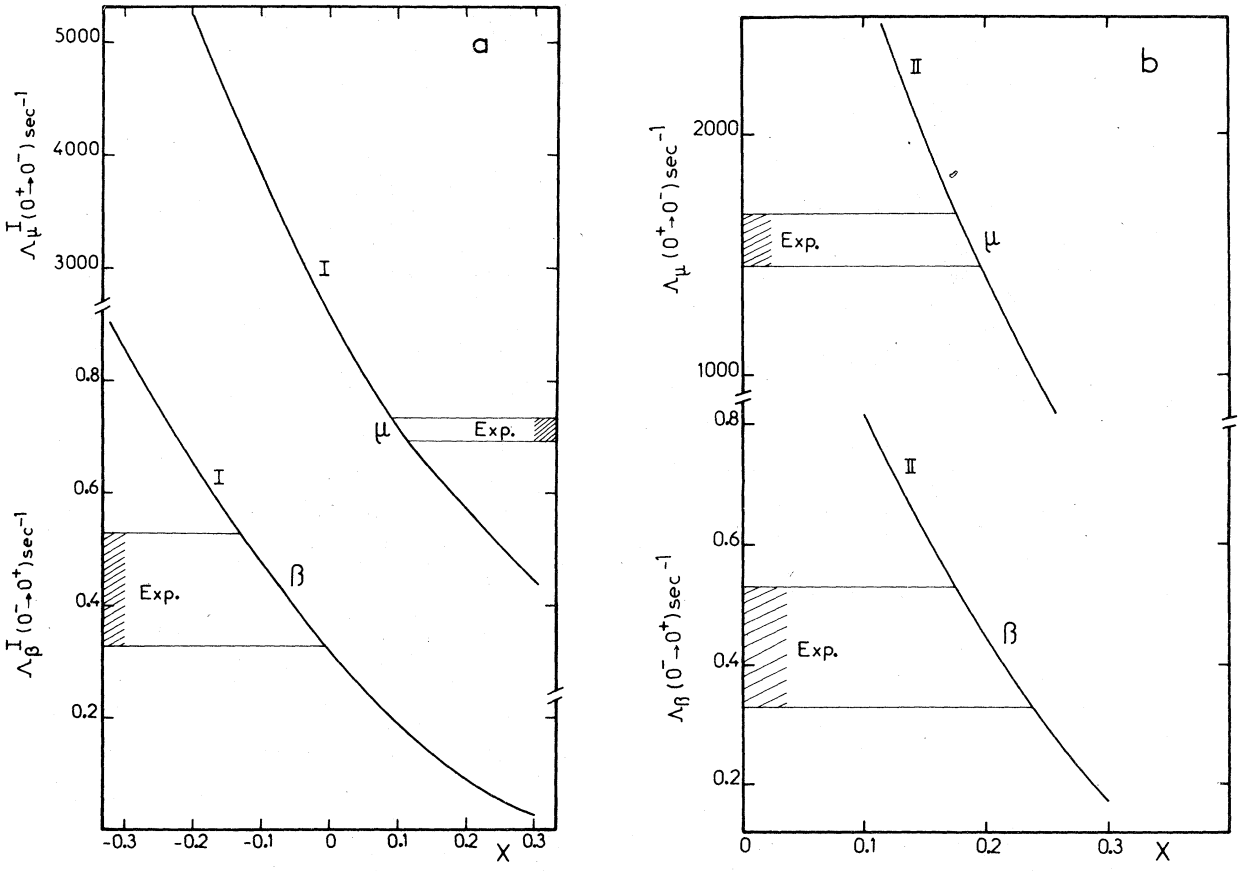

FIG. 12. Variation of $\Lambda_\mu(0^+ \to 0^-)$ and $\Lambda_\beta(0^- \to 0^+)$ as a function of mixing coefficient X. The theoretical curves I (part a) corresponds to the impulse approximation. The theoretical curves II (part b) include the mesonic exchange correction. The Saclay experimental capture rate and the Louvain experimental β-decay rate (Ref. 38) are illustrated as the experimental values.

over, it would be desirable to reproduce $\Lambda_\mu(0^+ \to 0^-)$ and $\Lambda_\beta(0^- \to 0^+)$ separately, rather than their ratio. It is perhaps significant that with OPE corrections it is possible to reproduce both experimental rates with a unique value of the mixing parameter X, contrary to the IA (Fig. 12). The very high X value ($\simeq 0.18$) found in Fig. 12(b) is perhaps in favor of high energy configuration mixing.

In conclusion the experimental rates we find for the $0^+ \to 1^-$ and $0^+ \to 0^-$ muon capture transitions are consistent with an apparently negligible breaking of the IA for the spacelike part of the weak axial current. The $0^+ \to 0^-$ muon transition rate, together with the inverse $0^- \to 0^+$ β-decay rate, can be interpreted, in a rather model independent way, by a strong effect of the OPE correction to the timelike part of the weak axial current. This might be the first confirmation of current algebra and PCAC in a weak process taking place in a complex nucleus.

ACKNOWLEDGMENT

We would like to thank Dr. J. Delorme and Dr. M. Rho for their constant interest from the beginning of this study and for fruitful discussions. We would also like to thank Dr. J. C. Philippot for his help in the calibration of the detector. Two of us (M. G. and P. G.) are very grateful to Dr. P. Catillon for his generous hospitality in the Nuclear Physics Department at Saclay. This work is part of the thesis of one of us (P. G.).

---

*Permanent address: INP, Université Claude Bernard, Lyon I, 43 bd. du 11 Novembre 1918, 69621 Villeurbanne, France.

[1]I. S. Shapiro and L. D. Blokhinstev, Zh. Eksp. Teor. Fiz. 39, 1112 (1960) [Sov. Phys.-JETP 12, 775 (1960)].
[2]T. Ericson, J. C. Sens and H. P. C. Rood, Nuovo Cimento 34, 51 (1964).
[3]V. Gillet and D. A. Jenkins, Phys. Rev. 140, B32 (1965).
[4]A. Fujii, M. Morita and Ohtsubo, Suppl. Prog. Theor. Phys. Extra Number 303 (1968).
[5]A. M. Green and M. Rho, Nucl. Phys. A130, 112 (1969).
[6]M. Rho, Phys. Rev. 161, 955 (1967).
[7]R. C. Cohen, S. Devons, and A. D. Kanaris, Nucl. Phys. 57, 255 (1964).
[8]A. Astbury, L. B. Auerbach, D. Cutts, R. J. Esterling, D. A. Jenkins, N. H. Lipman, and R. C. Scafer, Nuovo Cimento 33, 1021 (1964).
[9]J. P. Deutsch, L. Grenacs, J. Lehmann, P. Lipnik, and P. C. Macq, Phys. Lett. 29B, 66 (1969).
[10]F. R. Kane, M. Eckhause, G. H. Miller, R. L. Roberts, M. E. Vislay, and R. E. Welsh, Phys. Lett. 45B, 292 (1973).
[11]W. W. Givens, T. W. Bonner, Sheng Heng Fang, R. C. Bearse, and A. A. Rollefson, Nucl. Phys. 46, 504 (1963).
[12]L. Palffy, J. Lehmann, L. Grenacs, and M. Subotowicz, Nuovo Cimento 3A, 505 (1971).
[13]M. Eckhause, R. T. Siegel, R. E. Welsh, and T. A. Fillipas, Nucl. Phys. 81, 575 (1966).
[14]F. Ajzenberg-Selove, Nucl. Phys. A166, 1 (1971); A190, 1 (1972).
[15]P. Y. Bertin *et al.*, Internal Report No. DPh-N/HE 71-3, 1971 (unpublished).
[16]J. C. Philippot, I. E. E. E. Trans. Nucl. Sci. NS-17, 446 (1970).
[17]A. Suzuki, Phys. Rev. Lett. 19, 1005 (1967).
[18]F. J. Hartmann, T. von Egidy, R. Bugmann, M. Kleber, H. J. Pfeiffer, K. Springer, and H. Daniel, Phys. Lett. 37, 331 (1976).
[19]R. Bergmann, H. Daniel, F. J. Hartmann, J. J. Reidy, and W. Wilhelm, S. I. N. Newsletter 9, 40 (1977).
[20]H. Ayache, Internal Report, DPh-h/HE77-8, 1977 (unpublished).
[21]A. Gonçalves, B. Bihoreau, M. Griffon, P. Guichon, J. Julien, L. Roussel, and C. Samour (to be published).
[22]M. E. Plett and S. E. Sobottka, Phys. Rev. C 3, 1003 (1971); J. Wojtkowska, V. S. Evseyev, T. Kozlowski, T. N. Mamedov, and V. S. Roganov, Yad. Fiz. 14, 624 (1971) [Sov. J. Nucl. Phys. 14, 349 (1972)].
[23]P. Guichon, M. Giffon, J. Joseph, R. Laverrière, and C. Samour, Z. Phys. A285, 183 (1978).
[24]P. Guichon, M. Giffon, and C. Samour, Phys. Lett. B74, 15 (1978).
[25]A. Maksymowicz, Nuovo Cimento 48, 320 (1967).
[26]T. W. Donnelly and J. D. Walecka, Phys. Lett. B41, 275 (1972).
[27]M. Rho, Nucl. Phys. A231, 493 (1974).
[28]J. Delorme, M. Ericson, A. Figureau, and C. Thévenet, Ann. Phys. (N.Y.) 102, 273 (1976).
[29]M. Chemtob, in *Mesons in Nuclei*, edited by D. H. Wilkinson and M. Rho (to be published).
[30]M. Chemtob and M. Rho, Nucl. Phys. A163, 1 (1971).
[31]In fact for each transition, it would be more judicious to speak about multipole renormalization rather than coupling constant renormalization. Indeed the operators associated with the coupling constants do not span a complete orthogonal set of operators in the space of nuclear states.
[32]This procedure has been used essentially in nuclear matter because it makes simple the evaluation of pion rescattering effects when the Pauli principle is neglected or approximated. We emphasize that the results obtained in this way cannot be used directly. They must be modulated by the local density at which the transition occurs. Because the transition of interest here stand always at the nucleus surface, the results are strongly modified (Ref. 33). The unjustified use of ordinary nucleon matter density to evaluate these effects has been the origin of some confusion.
[33]J. Delorme and A. Figureau, Journées d'Etudes, La Toussuire, 1977 (unpublished).
[34]For completeness the value of the weak coupling constants used in the IA part are $g_v = 0.98$, $g_M = 3.61$, $g_A = 1.23$, $g_P = 7 g_A$. They are evaluated at muon capture transfer ($= 95$ MeV).
[35]S. L. Adler and Y. Dothan, Phys. Rev. 151, 1267 (1966).
[36]K. Kubodera, J. Delorme, and M. Rho, Phys. Rev. Lett. 40, 755 (1970).
[37]J. Delorme, private communication.
[38]L. Palffy, J. P. Deutsch, L. Grenacs, J. Lehmann, and M. Steels, Phys. Rev. Lett. 34, 212 (1975).